06

Phase transition and strength properties of eutectic lead-bismuth alloy in the temperature range of $20-110^\circ$C under shock loading

© A.S. Savinykh,[1,2] G.V. Garkushin,[1,2] S.V. Razorenov[1,2]

[1] Federal Research Center for Problems of Chemical Physics and Medical Chemistry, Russian Academy of Sciences, 142432 Chernogolovka, Moscow region, Russia
[2] Joint Institute for High Temperatures, Russian Academy of Sciences, 125412 Moscow, Russia
e-mail: savas@ficp.ac.ru

Received August 30, 2024
Revised November 12, 2024
Accepted November 18, 2024

The phase transition parameters of the samples of the eutectic alloy Bi — 56.5 mass%, Pb — 43.5 mass% 0.2−8 mm thick were measured at initial temperatures of 20, 60, 96 and 111°C and a maximum shock compression stress of ~ 4 GPa. In experiments, the structure of compression and rarefaction waves was recorded using the VISAR laser Doppler velocimeter. A decrease in the phase transition stress was revealed as the compression wave propagated through the sample, the initial and maximum transition rates were estimated and the times of the corresponding transformations were determined. The measurements of the values of the Hugoniot elastic limit and the spall strength at stresses above the phase transition stress were carried out.

Keywords: lead-bismuth eutectic alloy, shock waves, phase transition, temperature, Hugoniot elastic limit, spall strength.

DOI: 10.61011/TP.2025.01.60514.226-24

Introduction

Melts of lead with bismuth, mainly — eutectic alloy Bi — 56.5%, Pb — 43.5%, are used as coolants in special-purpose reactors and are considered as promising coolants for pulsed thermonuclear reactors. Studies of the thermophysical properties of liquid metal coolants began in the 1950s [1] and continue up to the present time [2–5]. The main component of the eutectic alloy is bismuth, which undergoes a phase transition from the Bi-I phase to the Bi-II phase at a pressure of 2.5−2.8 GPa [6–10] under the impact compression, in static loading conditions 2.55 GPa [11]. No phase transitions have been recorded in lead at pressures close to the pressure of the Bi-I-Bi-II phase transition in bismuth.

The range of maximum stresses of shock compression of samples was expanded to 4 GPa in this study In continuation of Ref. [12] to register the phase transformation in bismuth, which is part of the eutectic alloy. The objectives of this study are to evaluate the dependence of the kinetics of phase transformation on the initial temperature and to study the impact of phase transformation on the strength properties of a eutectic alloy in the temperature range up to melting point.

1. Material and test setup

The initial blanks of the eutectic alloy Bi(56.3%)−Pb(43.7%) were produced in a vacuum furnace in the form of cylinders with a diameter of 50 mm and a length of 150 mm in „Tinkom“ LLC, Kaluga, Russia. Plane-parallel samples with a thickness of 0.25−8 mm were cut from one blank by the electroerosion method followed by surface treatment (grinding and polishing). The density value ρ_0 measured by hydrostatic weighing was 10.660 g/cm^3. The density at elevated temperature was estimated from the ratio $\rho_0 = 10.52177 + 0.00046026T$ g/cm^3 ($273.17^\circ\text{C} < T < 397.8^\circ\text{C}$) [13]. The melting point T_m of the studied alloy is 124.8°C. The value of the longitudinal velocity of sound c_l was measured in Ref. [12] and amounted to 2200 ± 10 m/s. The value of the longitudinal velocity of sound is $c_l = 2100$ m/s at a temperature of 102°C according to Ref. [14]. Calculations of c_l at the temperatures of the experiments were performed by linear interpolation, since no features depending on the density and temperature [13] were found. The value of the volumetric speed of sound according to the data of Ref. [14] is $c_b = 1900$ m/s and varies insignificantly in the studied temperature range.

The shock wave loading of the studied samples was carried out by 0.2−5.5 mm thick copper impactor accelerated to a velocity of 330 ± 10 m/s using a 50 mm gas gun. The velocity and skew of the impactors were monitored only in experiments at room temperature using electrocontact sensors. The maximum skew of the impactor at the moment of impact did not exceed 0.5 mrad. The gun barrel and the space around the sample were vacuumed before the experiment. The samples were heated before impact loading by resistive heaters located at a distance of 2−2.5 mm from the sample surface. The design of the heater, made of fechral wire, ceramic straws and high-temperature glue based on aluminum oxide, made it possible to evenly heat the sample to the required temperature. The temperature was controlled by two chromel–alumel thermocouples. The difference between the thermocouple readings did not exceed 1–2°. The controlled heating rate of the sample was ~ 0.05–$0.1°$ s. The heating rate slowed down to $\sim 0.02°$ s as the test temperature approached. The velocity profile of the free surface of the sample $u_{fs}(t)$ was recorded in each experiment using VISAR [15] laser Doppler interferometric velocimeter with high spatial and temporal resolution. The interferometer constant was 168 m/s.

2. Results of measurements of velocity profiles of free surface

The measurement results in the form of velocity profiles of the free surface of samples of the eutectic BiPb alloy with a thickness of 0.2–8 mm at room temperature are shown in Fig. 1, *a*. The loading was carried out by a copper impactor at a velocity of 330 m/s. The output of an elastic wave propagating with the longitudinal speed of

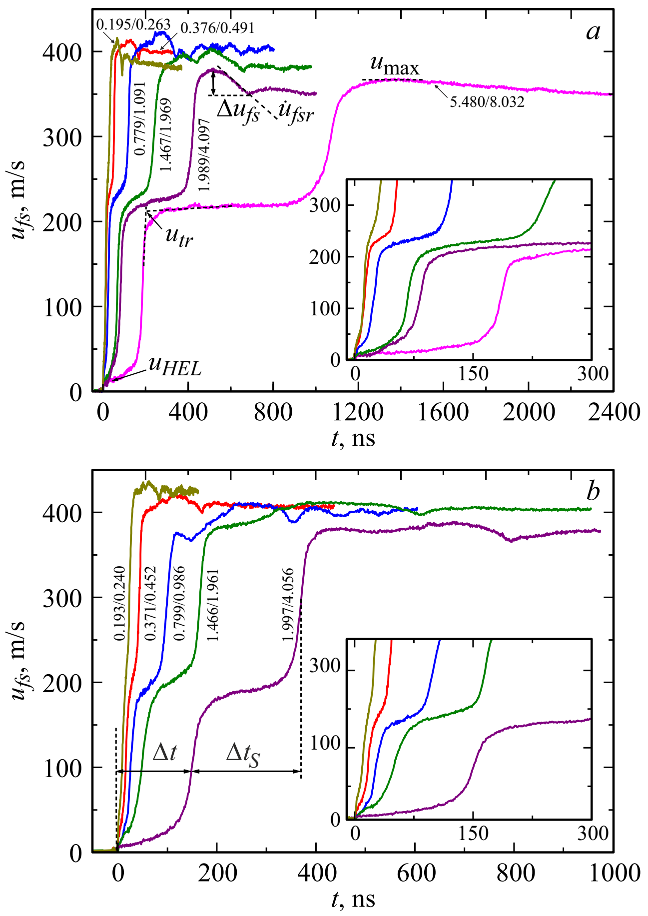

Figure 1. Free surface velocity profiles of samples of Bi–Pb alloy. The thickness of the impactor and the thickness of the sample are indicated for profiles. *a* — samples with thickness 0.2–8 mm at 20°C, *b* — samples with thickness 0.2–4 mm at 96°C.

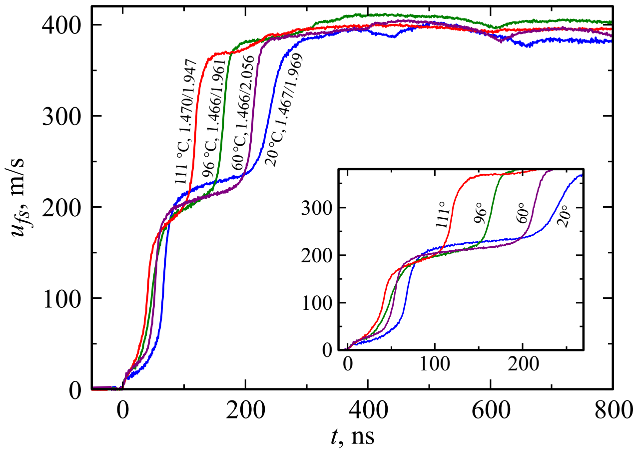

Figure 2. Free surface velocity profiles of Bi–Pb samples with a thickness of 2 mm at initial temperatures 20–111°C. The temperature, thickness of the impactor, and thickness of the sample are indicated for the profiles.

sound c_l and amplitude u_{HEL} is recorded on the profiles $u_{fs}(t)$. A propagation of a plastic wave with an amplitude of u_{tr} corresponding to the phase transformation in bismuth is recorded on the free surface after the elastic wave as well as the propagation of the second plastic wave with an amplitude of u_{max}. After reaching the maximum values of the velocity of the free surface, a decrease of velocity is recorded, associated with the surfacing of a part of the rarefaction wave. The amplitude of the rarefaction wave Δu_{fs} determines the spall strength of the studied material. A significant increase of the amplitude of the elastic precursor u_{HEL} is recorded on presented profiles $u_{fs}(t)$ with a decrease of sample thickness, which indicates the attenuation of the elastic precursor with the distance traveled and a slight attenuation of the first plastic wave having an amplitude u_{tr}. In addition, an increase of the amplitude of the deflection pulse Δu_{fs} is observed with a decrease of the sample thickness.

Fig. 1, *b* shows the velocity profiles of the free surface of the eutectic bismuth —lead alloy in the thickness range of 0.2–4 mm under the same loading conditions as the results shown in Fig. 1, *a*, but at the initial temperature of the samples of 96°C. The experiments performed at a temperature of 96°C demonstrated the same trends of the amplitudes of the elastic precursor, the attenuation wave, and the first plastic wave with the increase of the sample thickness as at room temperature.

Fig. 2 shows the profiles $u_{fs}(t)$ of samples of the Bi–Pb eutectic alloy with a thickness of 2 mm in the initial temperature range of 20–111°C. The effect of temperature on the amplitude of the elastic precursor u_{HEL} and the amplitude of the spallation pulse Δu_{fs} is insignificant, in contrast to its effect on the amplitude of the first plastic wave u_{tr}, limited by the beginning of the phase transformation. In addition, these experiments show a strong dependence of the velocity of the first and second plastic waves on the initial temperature.

3. Elastic-plastic and strength properties

The measurement of the amplitude of the elastic compression wave on the profile $u_{fs}(t)$ allows calculating the stress at the front of the elastic precursor or the Hugoniot elastic limit of the material σ_{HEL} using the ratio

$$\sigma_{HEL} = \rho_0 c_l u_{HEL}/2, \tag{1}$$

the Hugoniot elastic limit σ_{HEL} is related to the dynamic yield strength σ_T under one-dimensional deformation by the ratio

$$\sigma_T = 3/2\sigma_{HEL}(1 - c_b^2/c_l^2). \tag{2}$$

As seen in Fig. 1 and 2, an incident rarefaction wave propagates to the free surface of the sample after the shock wave, accompanied by a decrease of velocity recorded on the profile $u_{fs}(t)$. The interaction of rarefaction waves incident and reflected from the free surface leads to the generation of tensile stresses inside the sample. When the strength of the sample is exceeded, a spall crack forms, which is recorded on the velocity profile as the first minimum. The spall pulse recorded on the profile $u_{fs}(t)$ is the result of stress relaxation to zero at the moment of spallation, followed by propagation of compression waves in both directions.

In a linear approximation, the spall strength is calculated as

$$\sigma_{sp} = 1/2\rho_0 c_b(\Delta u_{fs} + \delta), \tag{3}$$

where δ is the correction for velocity profile distortion due to differences in the velocity of the spall pulse front and the velocity of the plastic part of the incident rarefaction wave in front of it [16,17]. The measurement of the rate of decay

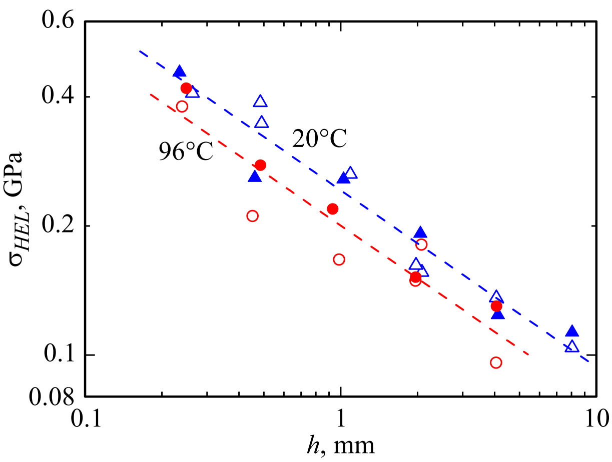

Figure 3. Dependences of the Hugoniot elastic limit σ_{HEL} on thickness h of sample of the eutectic alloy Bi–Pb at 20 and 96°C. Empty shape — at $\sigma_{\max} > \sigma_{tr}$, solid shape — at $\sigma_{\max} < \sigma_{tr}$ [12].

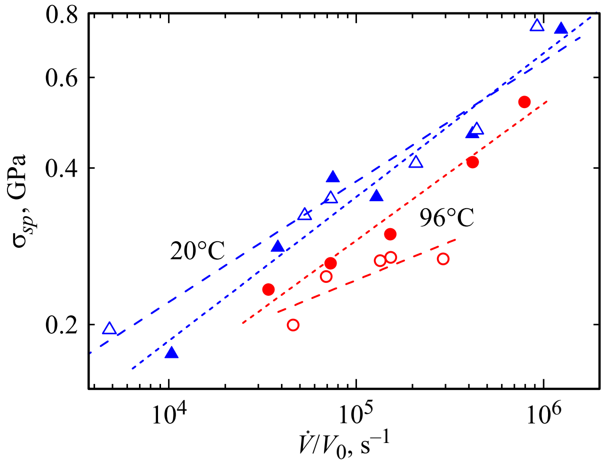

Figure 4. The dependence of the spall strength σ_{sp} on the strain rate in the rarefaction wave of alloy samples Bi–Pb at 20 and 96°C. Empty shape — at $\sigma_{\max} > \sigma_{tr}$, solid shape — at $\sigma_{\max} < \sigma_{tr}$ [12].

in the rarefaction wave $\dot{u}_{fsr}$ (Fig. 1, *a*) allows calculating the strain rate of the material before spallation using the ratio

$$\dot{V}/V_0 = -\dot{u}_{fsr}/2c_b. \tag{4}$$

The value $\dot{V}/V_0$ is actually the expansion rate of matter in the rarefaction wave.

Results of calculation of σ_{HEL} using the ratio (1) at initial temperatures of 20 and 96°C are summarized in Fig. 3. A strong dependence of the Hugoniot elastic limit on the distance traveled by the shock wave is recorded in both cases. The values of the Hugoniot elastic limit in experiments at the initial temperature of the samples 96°C are 20% lower than at room temperature in the measured range of sample thicknesses. Since the value of σ_{HEL} does not depend on the maximum compression stress, the data of study in Ref. [12] obtained at a maximum compression stress of 1.7 GPa, which is lower than the pressure of phase transformation, are added to Fig. 3. The dependences of σ_{HEL} on h at 20 and 96°C shown in Fig. 3 are approximated by a power function

$$\sigma_{HEL} = S(h/h_0)^{-\alpha}, \tag{5}$$

where $h_0 = 1$ mm, S is the coefficient with the value σ_{HEL} for $h_0 = 1$ mm, α is the exponent of power dependence. An increase of temperature to 96°C led to a decrease of the coefficient S to 200 MPa, while at room temperature $S = 243$ MPa. The power exponent α is the same for both 20°C and 96°C, and is equal to 0.41.

The values of spallation strength calculated using the ratio (3) and the values of strain rate in the rarefaction wave calculated using the ratio (4) for the eutectic alloy bismuth–lead at 20 and 96°C are presented as dependencies in Fig. 4. The data from Ref. [12] for a Bi–Pb eutectic alloy at maximum compression stresses

(~ 1.7 GPa) not exceeding the phase transformation stresses are added to the figure. There was no significant difference in the values of spall strength at room temperature like in the case of $\sigma_{\max} > \sigma_{tr}$ and $\sigma_{\max} < \sigma_{tr}$. The drop of spall strength was $\sim 20\%$ with an increase of the initial temperature of the samples 96°C at stresses $\sigma_{\max} < \sigma_{tr}$. Preheating of the sample to 96°C at $\sigma_{\max} > \sigma_{tr}$ resulted in a drop of spall strength by ~ 1.5 times compared to room temperature. Dependences σ_{sp} in the range of deformation rates $5 \cdot 10^3 - 2 \cdot 10^6\,\mathrm{s}^{-1}$ 1 presented in Fig. 4 are approximated by a power dependence in the form

$$\sigma_{sp} = A\left(\frac{\dot{V}/V_0}{\dot{\varepsilon}_0}\right)^{\beta}, \tag{6}$$

where $\dot{\varepsilon}_0 = 10^5\,\mathrm{s}^{-1}$, A is the coefficient with the value σ_{sp} for $\dot{\varepsilon}_0 = 10^5\,\mathrm{s}^{-1}$, β is the exponent of power dependence. The coefficient $A = 377$ MPa at room temperature and $\sigma_{\max} > \sigma_{tr}$, which is significantly higher than at 96°C, $A = 243$ MPa. $\beta = 0.233$ at initial temperature 20°C, its value decreases to 0.150 at 96°C. The coefficient β practically does not depend on temperature at $\sigma_{\max} < \sigma_{tr}$ and is 0.27 according to Ref. [12].

The values of the Hugoniot elastic limit σ_{HEL}, yield strength σ_T and spall strength σ_{sp} of 2 mm thick samples calculated using the ratios (1–3) at initial temperatures 20–111°C are summarized in Fig. 5. The experimental data shown in the figure are divided into two groups. One group are data when the component of the Bi-I alloy did not undergo transformation [12], the second group was obtained in this study at stresses $\sigma_{\max} < \sigma_{tr}$ and the other part of data were obtained in this work at $\sigma_{\max} > \sigma_{tr}$. The figure shows that the maximum compression stress does not affect the values of σ_{HEL} and σ_T in the temperature range of 20–111°C, since the elastoplastic transition occurs at

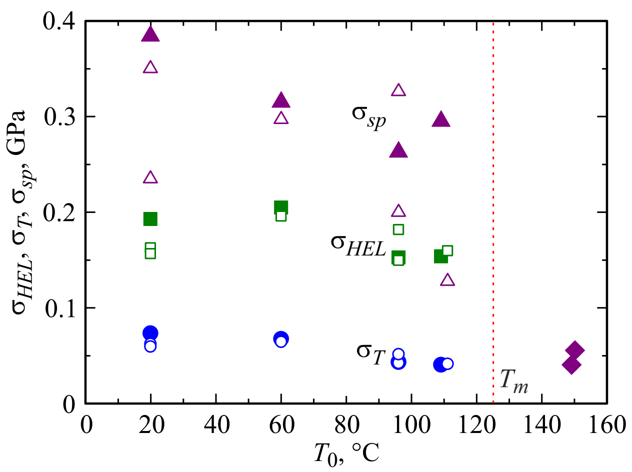

Figure 5. Dependences of the Hugoniot elastic limit σ_{HEL}, yield strength σ_T , and spall strength σ_{sp} of Bi–Pb alloy samples with a thickness of 2 mm on the initial temperature of the samples. Empty shape — at $\sigma_{\max} > \sigma_{tr}$, solid shape — at $\sigma_{\max} < \sigma_{tr}$ [12], T_m — melting point of the eutectic alloy. The values of the melt spall strength Bi–Pb at 150°C are taken from Ref. [14].

stresses lower than the phase transformation. A slight decrease of the above-mentioned characteristics of the material is recorded in case of an increase of temperature from room temperature to temperatures close to the melting point. The results of measurements of spall strength demonstrate the following. The spall strength values are higher at $\sigma_{\max} < \sigma_{tr}$ than at $\sigma_{\max} > \sigma_{tr}$ over the entire temperature range. The decrease of spall strength is insignificant in the range of maximum stresses $\sigma_{\max} < \sigma_{tr}$ as the sample temperature approaches the melting temperature of the alloy. An almost twofold decrease of strength is recorded in experiments at $\sigma_{\max} > \sigma_{tr}$ at temperatures near the melting point. This can be explained both by a change of the microstructure of the material after the phase transformation, and by additional heating of the material resulting from a more than twofold increase of the maximum compression stress.

4. Parameters and kinetics of phase transformation

The velocity profiles of the free surface of the eutectic alloy Bi–Pb, shown in Fig. 1, *a*, exhibit the splitting of a plastic wave associated with a phase transformation in bismuth. The stress at which the phase transformation occurs can be calculated by determining the amplitude of the first plastic wave u_{tr} using the ratio [18]:

$$\sigma_{tr} = \sigma_{HEL} + \rho_0 U_{S1}(u_{tr} - u_{HEL})/2, \tag{7}$$

where U_{S1} is the velocity of the first plastic wave. The following ratio was used to calculate the wave velocity U_{S1} [19]:

$$U_{S1} = c_l(h_s/c_l - \Delta t/2)/(h_s/c_l + \Delta t/2), \tag{8}$$

where Δt is the time difference between the propagation of the of the middle part of first plastic part of the compression wave and the elastic part of the compression wave to the free surface (Fig. 1, *b*), h_s is the sample thickness. The ratio (8) takes into account the interactions between incident and reflected waves near the free surface of the sample.

We use the ratio from Ref. [20] as a basis for calculating the wave velocity U_{S2}:

$$U_{S2} = U_{S1}(h_s/U_{S1} - \Delta t_s/2)/(h_s/U_{S1} + \Delta t_s/2), \tag{9}$$

where Δt_s is the time difference between the propagation to the free surface of the middle part of the second and first plastic compression waves (Fig. 1, *b*). The maximum compression stress exceeding the phase transformation stress was calculated using the ratio

$$\sigma_{\max} = \sigma_{tr} + \rho_{tr} U_{S2}(u_{\max} - u_{tr})/2, \tag{10}$$

where $\rho_{tr} = \rho_o U_{S2}/(U_{S2} - (u_{\max} - u_{tr})/2)$ is the density after the phase transformation.

Results of calculation using the ratio (7) the stresses of the phase transformation recorded on the free surface

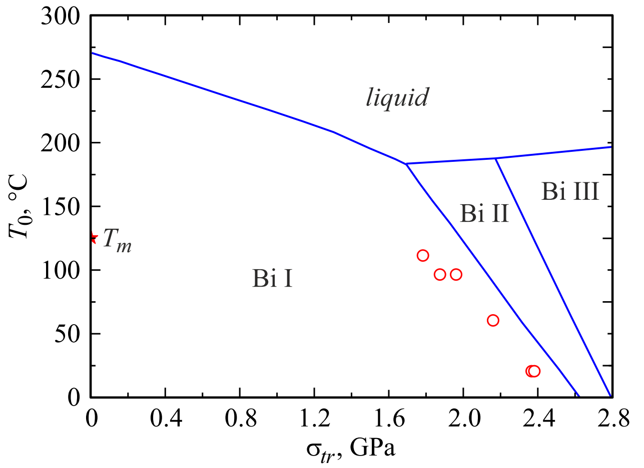

Figure 6. Dependence of the phase transformation stress on the initial temperature of samples of the eutectic alloy Bi–Pb with a thickness of 2 mm, T_m — melting point of the eutectic alloy. The bismuth phase diagram is taken from Ref. [9].

velocity profiles shown in Fig. 2 in the studied alloy are shown in Fig. 6. The phase diagram of bismuth has also been added to Fig. 6 [9]. 43.7% lead content in the studied alloy lowers the temperature and pressure of the Bi-I to Bi-II phase transition. The parameters of the phase transformation of the alloy are determined by the phase transformation in bismuth since there are no phase transitions in lead in this pressure and temperature range, according to literature sources. Fig. 6 shows that the phase transformation in the eutectic alloy occurs at lower stresses than the phase transformation of Bi-I to Bi-II in bismuth in the studied temperature range.

Fig. 7 shows the velocities of the first and second plastic waves of 2 mm thick samples of the eutectic bismuth alloy–lead calculated from the profiles $u_{fs}(t)$ shown in Fig. 2, depending on the initial temperature of the sample. The linear decrease of the speed of the first plastic wave as it approaches the melting temperature of the alloy is similar to the decrease of the longitudinal velocity of sound with the increase of the temperature [14] and is estimated at $\sim 5\%$. The velocity of the second plastic wave increases non-linearly by ~ 15–20% at the same time as it approaches the melting point. The almost linear decrease of the velocity of the first plastic wave and the nonlinear increase of the velocity of the second plastic wave with the increase of the temperature will continue until the melting point, when the two-wave configuration of the plastic wave disappears.

Fig. 8 shows the dependences of the phase transition stresses of the Bi–Pb alloy on the sample thickness at initial temperatures of 20 and 96°C obtained as a result of processing of profiles $u_{fs}(t)$ shown in Fig. 1. A comparison of the obtained dependences showed that the attenuation of the first plastic wave, determined by the relaxation of stresses behind its front due to phase transformation, weakly depends on the increase in thickness and practically does not depend on the initial temperature of the sample. Thus, the attenuation rate is estimated at 0.0098 GPa/mm at room temperature, it equals to 0.0076 GPa/mm at the initial temperature of 96°.

The obtained data on the attenuation of the first plastic wave at 20 and 96°C with the increase of sample thickness can be used to obtain a quantitative estimate of the initial transformation rate, as was done, for example, in the study with graphite [21] and armco-iron [18]. The initial rate of transformation $(\partial\alpha/\partial t)_h$ according to Ref. [21] can be estimated from the measured rate of attenuation of the first wave $d\sigma_{tr}/dh$ (Fig. 8) as

$$\left(\frac{\partial\alpha}{\partial t}\right)_h \approx \frac{2d\sigma_{tr}/dh}{(V_2 - V_1)\rho_0^2 U_{S1}}, \tag{11}$$

where V_1 and V_2 are the specific volumes of the initial and transformed matter, h is the Lagrangian coordinate. The specific volumes of the initial and con-

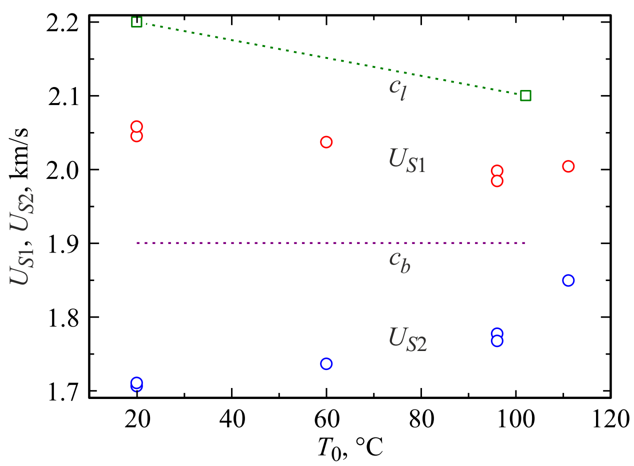

Figure 7. Dependences of the velocity of the first and second plastic waves of samples of eutectic alloy Bi–Pb with a thickness of 2 mm on initial temperature. The dependencies c_l and c_b on T_0 are taken from Ref. [14].

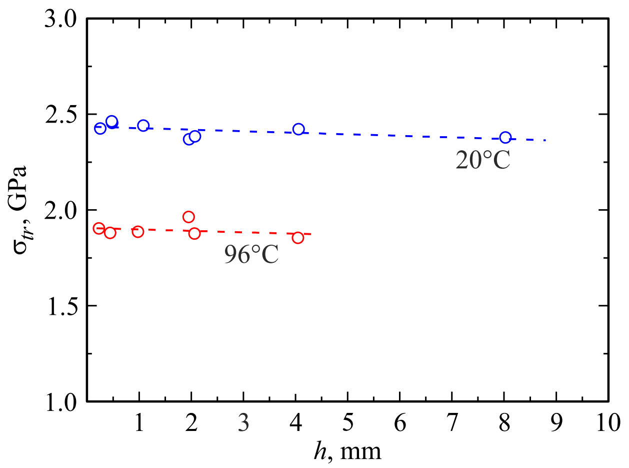

Figure 8. Dependences of phase transformation stresses σ_{tr} in eutectic alloy Bi–Pb at 20 and 96°C on sample thickness.

verted substances are defined as $V_1 = (U_{S1} - u_{tr}/2)/\rho_0 U_{S1}$, $V_2 = (U_{S2} - (u_{\max} - u_{tr})/2)/U_{S2}$.

We will estimate the maximum transformation rate, as was done in Ref. [21], by measuring acceleration in the second plastic wave on profiles $u_{fs}(t)$. The maximum compression rate is defined as $V_0^{-1} dV/dt = -(du_p/dt)/2U_{S2}$ for the obtained free surface velocity profiles (Fig. 2), where $-(du_p/dt) = \dot{u}_{fs2}$ is the maximum acceleration in the second plastic wave. Since compressibility in this region is determined mainly by the difference ΔV_f in the specific volumes of the phases of the initial and converted substances, the maximum transformation rates can be estimated as follows [21]:

$$\dot{\alpha} = V/\Delta V_f, \qquad (12)$$

where $\Delta V_f = V_2 - V_1$.

The respective transformation time [18] can be estimated using an estimate of the initial transformation rate (11) and the maximum transformation rate (12):

$$t_{tr} = 1/\dot{\alpha}. \qquad (13)$$

The initial rate of transformation and the maximum rate of transformation in the eutectic alloy Bi–Pb as a function of temperature, estimated using the ratios (11) and (12), is shown in Fig 9. The following figure shows that the maximum rate of transformation exceeds the initial rate of transformation by an order of magnitude. A slight decrease of the initial rate of transformation is recorded as the temperature increases, while the maximum transformation rate significantly increases. The maximum transformation rate is three times higher at 111°C compared to room temperature. The same trend is observed with the estimated transformation time obtained using the ratio (13) and shown in Fig. 10. The transformation time slightly increases at the initial transformation rate as the temperature increases. At the same time, a significant reduction of the transformation time at the maximum transformation rate is observed with the increase of the temperature. The difference between the transformation time at the maximum and initial transformation rates is more than an order of magnitude.

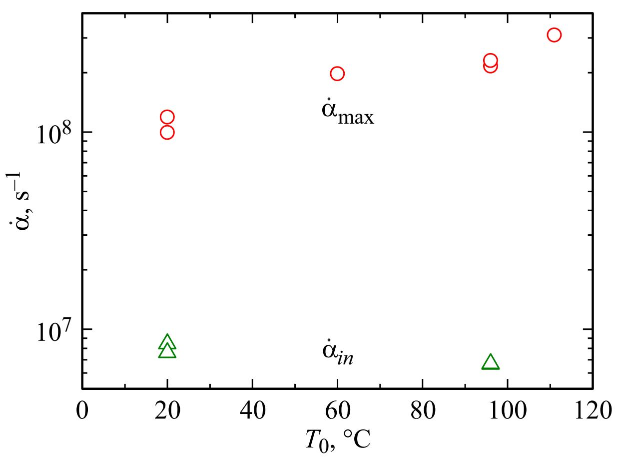

Figure 9. Initial $\dot{\alpha}_{in}$ and maximum $\dot{\alpha}_{\max}$ transformation rates in eutectic alloy Bi–Pb depending on temperature.

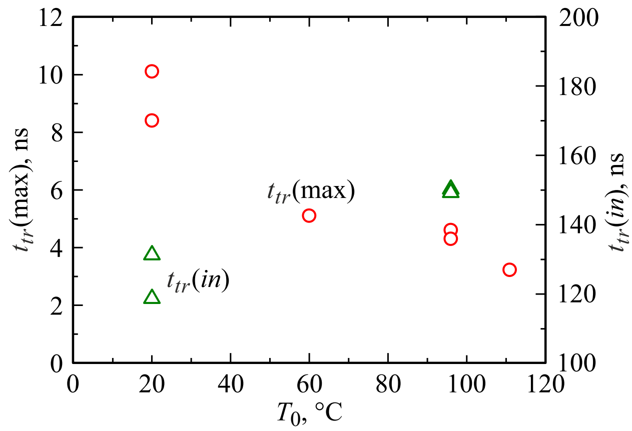

Figure 10. The time of phase transformation at the initial $t_{tr}(in)$ and maximum $t_{tr}(\max)$ transformation rates in eutectic alloy Bi–Pb as a function of temperature.

Conclusion

Experiments with shock wave loading of samples of eutectic alloy Pb–Bi (43.7/56.3) with a thickness of 0.2–8 mm at temperatures of 20, 60, 96 and 111°C and maximum compression stress of ~ 4 GPa. Were carried out the obtained velocity profiles of the free surface show the splitting of the plastic wave into two, associated with the phase transformation of Bi-I into Bi-II. The compression stress of the phase transformation at 20°C was 2.4 GPa with a further decrease to 1.78 GPa at 111°C. It is shown that the velocity of the second plastic wave increases with an increase of the initial temperature of the sample, while the velocity of the first plastic wave decreases. The attenuation of the phase transformation stress with thickness increase was revealed, the attenuation rate was 0.0098 GPa/mm at 20°C, the attenuation rate was 0.0076 GPa/mm at 96°C. The initial and maximum transformation rates of the studied eutectic alloy were estimated and the corresponding transformation times were estimated. A threefold increase of the rate of maximum transformation and a slight decrease of the initial rate of transformation were recorded in the temperature range of 20–111°C. At the same time, the transformation time at the maximum transformation rate decreases from 9 to 3 ns at temperatures of 20–111°C. The transformation time at the initial transformation rate increases from 120 ns at 20°C to 150 ns at 96°C. The phase transformation in bismuth significantly affected the strength properties of the studied alloy. The spall strength decreases almost threefold with temperature increase to 111°C at $\sigma_{\max} > \sigma_{tr}$, while it decreases by $\sim 30\%$ at $\sigma_{\max} < \sigma_{tr}$. A fourfold increase of spall strength is recorded in the studied range of strain rates both at $\sigma_{\max} > \sigma_{tr}$ and at $\sigma_{\max} < \sigma_{tr}$. An increase of temperature to 96°C led to a drop of spall strength by ~ 1.5 times compared to room temperature. The Hugoniot elastic limit and yield strength at stresses both below and above the phase transformation are weakly sensitive to temperature increases.

Funding

The work was performed as part of R&D under contract No. 17706413348210001380/226/3464-D dated June 22, 2021, using equipment from the Moscow Regional Explosive Center for Collective Use of the Russian Academy of Sciences as part of the State Assignment under the program glqq Comprehensive Study of Physico-Chemical Properties and Processes in Matter Under High-Energy Conditions", Topic No FFSG-2024-0001, reg. No. 124020600049-8. The samples were prepared in the Joint Institute for High Temperatures, RAS under a subsidy for the fulfillment of state assignment No. 075-00270-24-00.

Conflict of interest

The authors declare that they have no conflict of interest.

References

[1] S.S. Kutateladze, V.M. Borishansky, I.I. Novikov, O.S. Fedynsky. *Zhidkometallicheskie teplonositeli* (Atomizdat, M., 1958) (in Russian)
[2] V.S. Chirkin. *Teplofizicheskie svojstva materialov yadernoj tekhniki*, Spravochnik (Atomizdat, M., 1968) (in Russian).
[3] K. Morita, V. Sobolev, M. Flad. J. Nucl. Mater., **362**, 227 (2007). DOI: 10.1016/j.jnucmat.2007.01.048
[4] P.S. Popel', D.A. Yagodin, A.G. Mozgovoi, M.A. Pokrasin. High Temp, **48**, 181 (2010). DOI: 10.1134/S0018151X10020070
[5] V.P. Sobolev, P. Schuurmans, G. Benamati. J. Nucl. Mater., **376**, 358 (2008). DOI: 10.1016/j.jnucmat.2008.02.030
[6] Z. Rozenberg. J. Appl. Phys., **56** (11), 3328 (1984). DOI: 10.1063/1.333855
[7] R.E. Duff, F.S. Minshall. Phys. Rev., **108** (5), 1207 (1957). DOI: 10.1103/PhysRev.108.1207
[8] D.B. Larson. J. Appl. Phys., **38** (4) 1541 (1967). DOI: 10.1063/1.1709720
[9] J.R. Asay. J. Appl. Phys., **48**, 2832 (1977). DOI: 10.1063/1.324144
[10] M.N. Pavlovskii, V.V. Kommissarov. Sov. Phys. JETP, **83** (6), 2146 (1982).
[11] E.Y. Tonkov. *Fazovye prevrashcheniya soedinenij pri vysokom davlenii* (Metallurgiya, M., 1988), vol. 1. (in Russian).
[12] A.S. Savinykh, G.V. Garkushin, S.V. Razorenov. Tech. Phys., **68** (3), 3539 (2023). DOI: 10.21883/TP.2023.03.55809.269-22
[13] A.A. Aleksandrov, K.A. Orlov, V.F. Ochkov. *Svojstva i protsessy rabochikh tel i materialov atomnoj energetiki*(Izdat. dom MEI, M., 2012) (in Russian).
[14] G.V. Garkushin, A.S. Savinykh, G.I. Kanel, S.V. Razorenov. JETP, **128** (2), 268 (2019). DOI: 10.1134/S1063776119010114
[15] L.M. Barker, R.E. Hollenbach. J. Appl. Phys., **43**, 4669 (1972). DOI: 10.1063/1.1660986
[16] G.I. Kanel. Int. J. Fract., **163** (1), 173 (2010). DOI: 10.1007/s10704-009-9438-0
[17] G.I. Kanel. J. Appl. Mech. Tech. Ph. **42**, 358 (2001). DOI: 10.1023/A:1018804709273
[18] E.B. Zaretsky, G.I. Kanel. J. Appl. Phys., **117**, 195901 (2015). DOI: 10.1063/1.4921356
[19] G.I. Kanel, S.V. Razorenov, V.E. Fortov. *Shock-Wave Phenomena and Properties of Condensed Matter* (Springer, 2004)
[20] E.B. Zaretsky. J. Appl. Phys., **106**, 023510 (2009). DOI: 10.1063/1.3174442
[21] G.I. Kanel, G.S. Bezruchko, A.S. Savinykh, V.V. Milyavskii. K.V. Khishchenko. High Temp., **48**, 806 (2010). DOI: 10.1134/S0018151X10060064

Translated by A.Akhtayamov